2009-1370

47th AIAA Aerospace Science Meeting, 5-8 January 2009, Orlando, Florida

Calculation of Slow Invariant Manifolds for Reactive Systems

Ashraf N. Al-Khateeb*, Joseph M. Powers†, Samuel Paolucci‡,
Andrew J. Sommese§, and Jeffrey A. Diller¶

University of Notre Dame, Notre Dame, Indiana, 46556-5637, USA

One-dimensional slow invariant manifolds for dynamical systems arising from modeling unsteady, isothermal, isochoric, spatially homogeneous, closed reactive systems are calculated. The technique is based on global analysis of the composition space of the reactive system. The identification of all the system's finite and infinite critical points plays a major role in calculating the system's slow invariant manifold. The slow invariant manifolds are constructed by calculating heteroclinic orbits which connect appropriate critical points to the critical point which corresponds to the unique stable physical critical point of chemical equilibrium. The technique is applied to small and large detailed kinetics mechanisms for hydrogen combustion.

I. Introduction

In detailed kinetics models, the presence of a wide range of scales induces a large computational cost when calculations are fully resolved. Because direct numerical simulation (DNS) is not feasible for many practical flows, the main challenge in modeling is to simplify the problem without significant loss of accuracy. One of the major approaches employs lower dimensional manifolds,[1] which are based on a reduction in the composition space dimension.

For spatially homogeneous systems, reaction dynamics are described by a set of ordinary differential equations (ODEs). The solutions of this set of ODEs are represented by trajectories in the species composition space. Each trajectory represents the reactive system's evolution with time for a specific initial condition. The evolved trajectories seem to quickly be attracted to a special trajectory and stay exponentially close to it until they reach equilibrium in infinite time.[2] The reactive system's slow modes are the only active ones on this special trajectory. Thus, identifying this slow invariant manifold (SIM) for a reactive system will make it possible to reduce the computational cost by filtering the system's fast modes. For each reactive system there are SIMs of different dimensions; this work focus on constructing only one-dimensional (1-D) SIMs.

Here, 1-D SIMs for unsteady spatially homogeneous mixtures of calorically imperfect ideal gases described by detailed kinetics are calculated. While such construction has been done for small two-dimensional model systems,[3,4] the present work offers the first construction of a SIM for a realistic detailed kinetics system of greater than two dimensions. We note that here dimensionality refers to the dimension of the composition space and not to the ordinary spatial dimension, as the systems we consider have no spatial inhomogeneity. The SIM is constructed by a global analysis over the entire composition space. By finding all equilibria and connecting them via heteroclinic orbits, it is easy to identify the system's actual SIM. Detailed hydrogen-air kinetic systems will be the focal mechanisms of this paper. These systems are of interest since they are intrinsic to common combustion applications, included in the combustion of all hydrocarbons, and are well-known and widely accepted.

*Ph.D. Candidate, Department of Aerospace and Mechanical Engineering, AIAA Student Member, aalkhate@nd.edu.
†Professor, Department of Aerospace and Mechanical Engineering, AIAA Associate Fellow, powers@nd.edu.
‡Professor, Department of Aerospace and Mechanical Engineering, AIAA Member, paolucci@nd.edu.
§Professor, Department of Mathematics, sommese@nd.edu.
¶Associate Professor, Department of Mathematics, jdiller@nd.edu.

In comparison to other dimension reduction techniques that obtain approximate SIMs, such as the intrinsic low-dimensional manifold (ILDM),[5] the computational singular perturbation (CSP),[6] the invariant constrained equilibrium edge preimage curve method (ICE-PIC),[7] and the iterative method,[8] the technique presented here identifies the actual SIMs. In the first section, the governing ODEs for closed, isothermal, isochoric, reactive system are presented. This is followed by a reduction of the ODEs into a system of differential algebraic equations (DAEs) which describes the system's evolution within the reduced composition space. Following a brief description of how we identify and examine all the system's finite and infinite equilibria, the numerical method to construct the SIMs is presented. For the main result of this study, the 1-D SIMs for two realistic detailed kinetics isothermal reactive systems are calculated. Once the difficult task of identifying all of the equilibria is complete, it is seen that constructing the actual SIMs is easy and computationally efficient.

II. Mathematical Model

II.A. Governing Equations

We consider a mixture of total mass m confined in a constant volume V containing N gas phase species composed of L atomic elements that undergo J reversible reactions. The evolution is obtained from the following set of ODEs:[9]

$$\frac{dn_i}{dt} = V\dot{\omega}_i, \quad i = 1, \ldots, N. \tag{1}$$

Here, the independent variable is time t, and the dependent variables are the species' number of moles n_i. Also, $\dot{\omega}_i$ is species i's molar production rate per unit volume calculated using the following constitutive equations:[10]

$$\dot{\omega}_i = \sum_{j=1}^{J} \nu_{ij} A_j \; T^{\beta_j} \; \exp\left(\frac{-E_j}{\Re T}\right) \left(\prod_{i=1}^{N} \left(\frac{n_i}{V}\right)^{\nu'_{ij}} - \frac{1}{K_j^c} \prod_{i=1}^{N} \left(\frac{n_i}{V}\right)^{\nu''_{ij}} \right), \quad i = 1, \ldots, N, \tag{2}$$

$$K_j^c = \left(\frac{p^o}{\Re T}\right)^{\sum_{i=1}^{N} \nu_{ij}} \exp\left(-\frac{\sum_{i=1}^{N} \bar{\mu}_i^o \nu_{ij}}{\Re T}\right), \quad j = 1, \ldots, J. \tag{3}$$

Equations (2-3) are expressions of the molar species evolution rate per unit volume of species i using the Arrhenius reaction rate and the equilibrium constant of reaction j, respectively. In these equations, T is the constant mixture temperature, $\Re = 8.314 \times 10^7 \; erg \; mol^{-1} K^{-1}$ is the universal gas constant, and $\bar{\mu}_i^o$ is the constant molar-basis chemical potential of species i at standard pressure. Also, for each reaction from $j = 1, \ldots, J$, the quantities K_j^c, A_j, β_j, E_j, and ν_{ij} represent the equilibrium constant, the collision frequency factor, the temperature-dependent exponent, the activation energy, and the net stoichiometric coefficient for the i^{th} species, respectively. Moreover, $p^o = 1 \; atm$ is the reference pressure, ν'_{ij} and ν''_{ij} are the stoichiometric coefficients denoting the number of moles of reactants and products, respectively, with $\nu_{ij} = \nu''_{ij} - \nu'_{ij}$.

Also, we will need the thermal state equation for an ideal gas mixture,

$$p = \frac{\Re T}{V} \sum_{i=1}^{N} n_i, \tag{4}$$

where p is the mixture pressure.

II.B. Reduced System

The complete system, Eq. (1), defines an N-dimensional composition space. The dimensionality of this space is reduced by $L + Q$ as a consequence of 1) the conservation of L elements, and 2) any Q additional constraints that could possibly arise. As a result, the reactive system described by Eq. (1) is recast as an autonomous standard dynamical system of the form

$$\frac{dz_i}{dt} = f_i(z_1, \ldots, z_{N-L-Q}), \quad i = 1, \ldots, N - L - Q, \tag{5}$$

where $z_i = n_i/m$ are the species specific moles, and f_i is a set of non-linear coupled polynomials of degree `d` connected with a given reaction mechanism. Reactive system solutions are trajectories that move on the

reduced composition space $\mathbb{R}^{N-L-Q}$ which is a subspace of the full composition space $\mathbb{R}^N$. Full details are given by Al-Khateeb *et al.*[11]

III. Method

The proposed construction method of a reactive system's SIM is based on identifying all the equilibria of the ODEs that describe the species evolution, Eq. (5). In general, the set of equilibria of such functions is complex. Moreover, as demonstrated by Perko,[12] some of the dynamical system's equilibria are located at infinity. In this work, only the system's real isolated finite and infinite equilibria are considered.

III.A. Equilibria

To find the dynamical system's finite equilibria, we solve the algebraic problem $f_i(z_1, \ldots, z_{N-L-Q}) = 0$. One of these finite equilibria is the unique critical point located inside the physically accessible domain.[13] The rest of the finite equilibria are non-physical since at least one of the species mole numbers is negative, $n_i < 0$. Then, the dynamic behavior of the system in the neighborhood of each finite equilibrium is investigated by employing standard linearization techniques,

$$\frac{d}{dt}\left(z_i - {z_i}^e\right) \approx J^e_{ij}\left(z_j - {z_j}^e\right), \quad i = 1, \ldots, N-L-Q, \quad j = 1, \ldots, N-L-Q, \tag{6}$$

where quantities with superscript $(^e)$ are at the equilibrium state. Here, $J^e_{ij} = \partial f_i/\partial z_j|_{\mathbf{z}^e}$ is the constant Jacobian matrix evaluated at an equilibrium point. The stability of each critical point is determined by examining the eigenvalue spectrum λ_i of its local Jacobian and the corresponding eigenvectors υ_i. The local time scales over which the dynamical system, Eq. (6), evolves are given by the reciprocal of the real part of the system's eigenvalues, $1/|Re(\lambda_i)|$. In general, the dynamical system's eigenvalues are complex, where the reciprocal of the real parts provides the scales of the amplitude growth, and the reciprocal of the imaginary parts represents the period of oscillations. For the physical equilibrium point, the ratio between its largest and smallest time scales identifies the system's stiffness. In addition, the eigenvector associated with the smallest eigenvalue represents the system's slowest mode or direction in composition space along which the trajectories approach the equilibrium.

The next step is to identify the system's infinite equilibria. To do so, the projective space method is employed.[14] This technique maps the infinite critical points onto the finite domain, and it is realized by the following relations

$$Z_k = \frac{1}{z_k}, \qquad k \in \{1, \ldots, N-L-Q\}, \tag{7}$$

$$Z_i = \frac{z_i}{z_k}, \qquad i \neq k, \quad i = 1, \ldots, N-L-Q, \tag{8}$$

where z_k is any arbitrarily selected dependent variable, and $Z_i, i = 1, \ldots, N-L-Q$, are the state variables in the projective space. By employing the projective space mapping, the original dynamical system, Eqs. (5), is recast in the following form

$$\frac{dZ_i}{d\tau} = F_i\left(Z_1, ..., Z_{N-L-Q}\right), \quad i = 1, \ldots, N-L-Q, \tag{9}$$

where F_i is a set of non-linear functions that correspond to the non-linear functions f_i in the projective space, and τ is the transformed time in the projective space which is related to the time in the original space by the following relation,

$$\frac{dt}{d\tau} = \left(Z_k\right)^{\mathfrak{d}-1}. \tag{10}$$

The finite critical points of the resulting dynamical system with $Z_k = 0$ represent the infinite equilibria of the original system, Eq. (5).

III.B. Construction Method

The procedure for constructing the reactive system's SIM is summarized in these steps. After identifying all the equilibria, finite and infinite, the equilibria with at least one unstable mode are considered. Starting from

each one of these equilibria, a heteroclinic orbit is generated along its unstable mode. Only the generated orbits that connect to the physical equilibrium are considered. Among these orbits, two orbits represent the two branches of the system's 1-D SIM. These two orbits can be identified since they are the only ones that approach the physical equilibrium point in the direction of its slowest mode. The procedure for constructing a 1-D SIM can be systematically extended to construct higher-dimensional SIMs. Full details are given by Al-Khateeb *et al.*[11]

III.C. Computational Method

The kinetic rates and the thermodynamic properties are calculated using the public domain edition of the `CHEMKIN` package.[15,16] The typical computational time to construct a 1-D SIM is less than one minute on a 2.16 GHz Mac Pro machine. All the calculations have been performed to high precision. However, all the listed results are rounded to two significant digits. Integers indicate that the reported numbers are exact. Also, Bertini,[17] a *C*-code based on homotopy continuation, is used to obtain the system's equilibria to any desired accuracy. Moreover, all trajectories are obtained by numerical integration of the species evolution equations using a computationally inexpensive explicit fourth-order Runge-Kutta scheme.

IV. Results

IV.A. Simple Hydrogen-Oxygen Mechanism

Here, the method is illustrated using a simple but realistic system, the Michael mechanism[18] for the oxidation of hydrogen. This mechanism contains $N = 6$ species, $L = 2$ elements, and $J = 8$ elementary reactions; see Table 1. The chosen mixture temperature and volume are $T = 1200\ K$ and $V = 10^3\ cm^3$. The initial number of moles of all species are $n_i^* = 10^{-3}\ mol, i = 1, \ldots, N$. Thus, the initial mixture pressure is $p^* = 0.59\ atm$.

In this system, the total number of moles remain constant, as a consequence of the fact that the kinetics mechanism includes only bimolecular reactions. Consequently, one algebraic constraint, in addition to element conservation, is provided to the system: $Q = 1$. Thus, the reactive system is described in the $N - L - Q = 3$ dimensional reactive composition space,

$$\frac{dz_i}{dt} = f_i(z_1, z_2, z_3), \quad i = 1, 2, 3. \tag{11}$$

Here, $i = \{1, 2, 3\}$ corresponds to the species $\{H_2, O, O_2\}$, respectively. The rest of the species are given by the system's constraints. The full time evolution of species is shown in Fig. 1. The multi-scale nature of this system is clearly shown. Also, it can be visually noted that the times at which the first reaction event commences and that at which the system relaxes onto its chemical equilibrium are approximately $t = 10^{-9}\ s$ and $t = 10^{-4}\ s$, respectively.

The dynamical system, Eq. (11), has six finite critical isolated points,

$$\begin{aligned}
R_1 &= (z_1^e, z_2^e, z_3^e) = \left(-5.84 \times 10^{-2}, 6.85 \times 10^{-4}, -3.52 \times 10^{-4}\right)\ mol/g,\\
R_2 &= (z_1^e, z_2^e, z_3^e) = \left(4.65 \times 10^{-2}, 0, 3.49 \times 10^{-2}\right)\ mol/g,\\
R_3 &= (z_1^e, z_2^e, z_3^e) = \left(3.73 \times 10^{-3}, 6.32 \times 10^{-3}, 1.61 \times 10^{-2}\right)\ mol/g,\\
R_4 &= (z_1^e, z_2^e, z_3^e) = \left(6.33 \times 10^{-3}, -1.86 \times 10^{-3}, 2.49 \times 10^{-2}\right)\ mol/g,\\
R_5 &= (z_1^e, z_2^e, z_3^e) = \left(1.28 \times 10^{-3}, -5.98 \times 10^{-2}, 6.00 \times 10^{-2}\right)\ mol/g,\\
R_6 &= (z_1^e, z_2^e, z_3^e) = \left(1.43 \times 10^{-3}, -7.58 \times 10^{-2}, 7.08 \times 10^{-2}\right)\ mol/g.
\end{aligned}$$

It is clear that R_1, R_4, R_5 and R_6 are non-physical equilibria. Moreover, R_2 is also a non-physical critical point; this can be shown by computing the other species using the system's constraints. Thus, R_3 is the system's unique physical equilibrium point, consistent with the results in Fig. 1. Figure 2 shows part of the system's finite composition space, the physically accessible domain within the dashed simplex, and the finite equilibria. It is clear that R_3 is the only critical point inside the physically accessible domain.

The dynamical behavior analysis within the neighborhood of each critical point reveals that R_1, R_2, and R_5 are saddles, R_4 and R_6 are sources, and R_3 is a sink. The system's eigenvalues associated with each finite

critical point are:

$$\begin{aligned}
R_1 &: (\lambda_1,\lambda_2,\lambda_3) = (5.93\times10^6 \pm i5.10\times10^5, -1.18\times10^6)\ 1/s,\\
R_2 &: (\lambda_1,\lambda_2,\lambda_3) = (-1.01\times10^7, -3.35\times10^6, 7.93\times10^5)\ 1/s,\\
R_3 &: (\lambda_1,\lambda_2,\lambda_3) = (-1.02\times10^7, -1.23\times10^6, -4.30\times10^5)\ 1/s,\\
R_4 &: (\lambda_1,\lambda_2,\lambda_3) = (6.88\times10^6, 3.51\times10^6, 1.57\times10^6)\ 1/s,\\
R_5 &: (\lambda_1,\lambda_2,\lambda_3) = (5.65\times10^7, 3.56\times10^6, -1.06\times10^4)\ 1/s,\\
R_6 &: (\lambda_1,\lambda_2,\lambda_3) = (7.19\times10^7, 4.47\times10^6, 1.05\times10^4)\ 1/s.
\end{aligned}$$

In addition to the system's finite equilibria, Eq. (11) has three infinite equilibria. They are obtained using the projective space method, in which we select $k = 2$ arbitrarily. These equilibria are:

$$\begin{aligned}
I_1 &= (Z_1^e, Z_2^e, Z_3^e) = (-9.77, 0, -4.59)\,,\\
I_2 &= (Z_1^e, Z_2^e, Z_3^e) = (0.60, 0, -0.48)\,,\\
I_3 &= \left(Z_1^e, Z_2^e, Z_3^3\right) = (-0.01, 0, -0.67)\,.
\end{aligned}$$

The eigenvalue spectra of these critical points are:

$$\begin{aligned}
I_1 &: (\lambda_1,\lambda_2,\lambda_3) = (-5.74\times10^{12} \pm i7.83\times10^{12}, 6.10\times10^{12})\ g/(mol\ s),\\
I_2 &: (\lambda_1,\lambda_2,\lambda_3) = (-1.19\times10^{13}, 7.35\times10^{11}, 6.32\times10^{11})\ g/(mol\ s),\\
I_3 &: (\lambda_1,\lambda_2,\lambda_3) = (-1.12\times10^{13}, -6.50\times10^{11}, 7.62\times10^{9})\ g/(mol\ s).
\end{aligned}$$

All of the dynamical system's infinite equilibria are saddles.

Now, among the system's equilibria, the eigenvalue spectra of three critical points contain only one unstable direction (*i.e.* positive eigenvalue). These equilibria are R_2, I_1 and I_3.To construct the SIM, the dynamical system is numerically integrated, starting from these three critical points, in the direction of the unstable mode. Subsequently, three heteroclinic orbits are generated; two of these orbits connect to the physical equilibrium along its slowest mode. Thus, they represent the two branches of the 1-D SIM. These two heteroclinic orbits are the ones that start from R_2 and I_3. In Fig. 3, the 1-D SIM for the reactive system is shown. The attractiveness of the SIM is revealed by visually examining the relaxation of several trajectories onto it.

IV.B. Detailed Hydrogen-Air Mechanism

In this section, the 1-D SIM for a detailed kinetics hydrogen-air reactive system is constructed using the previously discussed technique. The used reaction mechanism is adopted from Miller *et al.*,[19] and it consists of $J = 19$ reversible reactions that describe how $N = 9$ species composed of $L = 3$ elements react, see Table 2.

The stoichiometric hydrogen-air mixture is initially at $p^* = 10^7\ dyne/cm^2$ and the chosen mixture temperature is $T = 1500\ K$. Because this system does not conserve the total number of moles, $Q = 0$. The reactive system can be described by the following $N - L = 6$ ODEs,

$$\frac{dz_i}{dt} = f_i(z_1, \ldots, z_6), \quad i = 1, \ldots, 6, \tag{12}$$

where the dependent variables are $\{z_{H_2}, z_{O_2}, z_H, z_O, z_{OH}, z_{H_2O}\}$, which correspond to $\{z_1, z_2, z_3, z_4, z_5, z_6\}$, respectively.

To construct the system's 1-D SIM, first all the system's isolated equilibria, finite and infinite, are found. Using the procedure discussed earlier, 326 finite and infinite equilibria are found. One of these critical points represents the physical equilibrium state. This point is

$$\begin{aligned}
R_{19} &= (z_1^e, z_2^e, z_3^e, z_4^e, z_5^e, z_6^e)\\
&= \left(1.98\times10^{-6}, 9.00\times10^{-7}, 1.72\times10^{-9}, 2.67\times10^{-10}, 3.66\times10^{-7}, 1.44\times10^{-2}\right)\ mol/g.
\end{aligned}$$

Then, the dynamical character of each of the real finite and infinite critical points is determined. It is found that among them there are only 14 critical points which have eigenvalue spectra that contain only one

unstable direction. All of these 14 equilibria are finite. Finally by examining all the trajectories that emanate from these 14 equilibria, only two of them are connected with R_{19} along its slowest mode via heteroclinic orbits. These two critical points are:

$$\begin{aligned} R_{74} &= (z_1^e, z_2^e, z_3^e, z_4^e, z_5^e, z_6^e) \\ &= \left(6.26 \times 10^{-5}, 3.43 \times 10^{-5}, -2.30 \times 10^{-6}, 4.80 \times 10^{-7}, -1.54 \times 10^{-5}, 1.44 \times 10^{-2}\right)\ mol/g, \\ R_{79} &= (z_1^e, z_2^e, z_3^e, z_4^e, z_5^e, z_6^e) \\ &= \left(-3.34 \times 10^{-6}, -1.50 \times 10^{-6}, 5.27 \times 10^{-9}, 8.82 \times 10^{-10}, -6.66 \times 10^{-7}, 1.44 \times 10^{-2}\right)\ mol/g. \end{aligned}$$

Figure 4 shows a 3-D projection of the 1-D SIM embedded inside the 6-D composition space. Since only the slow modes are present on the SIM, this 1-D manifold is the best description of the system's slowest dynamics.

V. Conclusion

Actual 1-D SIMs for closed, spatially homogenous, isothermal, reactive systems described by detailed kinetics are obtained. The construction method is based on a geometrical approach that relies upon finding and examining the dynamical behavior of all the system's critical points. It has been shown that the construction of the 1-D SIMs are algorithmically easy and computationally efficient. The resulting procedure provides a useful tool to significantly reduce the computational cost associated with modeling reactive systems.

Acknowledgments

The authors recognize the support of the National Science Foundation (NSF) under $CBET$-0650843, and the Center for Applied Mathematics at University of Notre Dame (CAM). Andrew J. Sommese is supported by NSF grants DMS-0410047 and DMS-0712910. Also, Jeffrey A. Diller is supported by NSF grant DMS-0653678.

References

[1]Singh, S., Powers, J. M., and Paolucci, S., "On Slow Manifolds of Chemically Reactive Systems," *Journal of Chemical Physics*, Vol. 117, No. 4, 2002, pp. 1482-1496.

[2]Lam, S. H., and Goussis, D. A., "Understanding Complex Chemical Kinetics with Computational Singular Perturbation," *Proceedings of the Twenty-second Symposium (International) on Combustion*, Combustion Institute, Pittsburgh, PA, 1988, pp. 931-941.

[3]Davis, M. J., and Skodje, R. T., "Geometric Investigation of Low-Dimensional Manifolds in Systems Approaching Equilibrium," *Journal of Chemical Physics*, Vol. 111, No. 3, 1999, pp. 859-874.

[4]Creta, F., Adrover, A., Cerbelli, S., Valorani, M., and Giona, M., "Slow Manifold Structure in Explosive Kinetics. Bifurcations of Points-at-Infinity in Prototypical Models," *Journal of Physical Chemistry A*, Vol. 110, No. 50, 2005, pp. 13447-13462.

[5]Maas, U., and Pope, S. B., "Simplifying Chemical Kinetics: Intrinsic Low-Dimensional Manifolds in Composition Space," *Combustion and Flame*, Vol. 88, No. 3-4, 1992, pp. 239-264.

[6]Lam, S. H., "Using CSP to Understand Complex Chemical Kinetics," *Combustion Science and Technology*, Vol. 89, No. 5-6, 1993, pp. 375-404.

[7]Ren, Z., Pope, S. B., Vladimirsky, A., and Guckenheimer, J. M., "The Invariant Constrained Equilibrium Edge Preimage Curve Method for The Dimension Reduction of Chemical Kinetics," *Journal of Chemical Physics*, Vol. 124, No. 11, 2006, p. 114111.

[8]Roussel, M. R., and Fraser, S. J., "On The Geometry of Transient Relaxation," *Journal of Chemical Physics*, Vol. 94, No. 11, 1991, pp. 7106-7113.

[9]Prigogine, I., and Defay, R., *Chemical Thermodynamics*, Longmans, London, 1954.

[10]Law, C. K., *Combustion Physics*, Cambridge University Press, New York, 2006.

[11]Al-Khateeb, A. N., Powers, J. M., Paolucci, S., Sommese, A. J., Diller, J. A., Hauenstein, J. D., Mengers, J. D., "Constructing Slow Invariant Manifolds for Closed Reactive Systems," *Journal of Chemical Physics*, to be submitted for publication.

[12]Perko, L., *Differential Equations and Dynamical Systems*, Springer, New York, 2001.

[13]Powers, J. M., and Paolucci, S., "Uniqueness of Chemical Equilibria in Ideal Mixtures of Ideal Gases," *American Journal of Physics*, Vol. 76, No. 9, 2008, pp. 848-855.

[14]Andronov, A. A., Leontovich E. A., Gordon, I. I., and Maier, A. G., *Qualitative Theory of Second Order Dynamical Systems*, John Wiley, New Work, 1973.

[15]Kee, R. J., Rupley, F. M., and Miller, J. A., "Chemkin-II: A Fortran Chemical Kinetics Package for the Analysis of Gas Phase Chemical Kinetics," Sandia National Labs., Rept. SAND89-8009B, Livermore, CA., 1992.

[16]Kee, R. J., Rupley, F. M., and Miller, J. A., "The Chemkin Thermodynamic Data Base," Sandia National Labs., Rept. SAND87-8215B, Livermore, CA., 1992.

[17]Bates, D. J., Hauenstein, J. D., Sommese, A. J., and Wampler, C. W., "Bertini: Software for Numerical Algebraic Geometry," Online available: http://www.nd.edu/∼sommese/bertini.

[18]Michael, J. V., "Measurement of Thermal Rate Constants by Flash or Laser Photolysis in Shock Tubes: Oxidations of H_2 and D_2," *Progress in Energy and Combustion Science*, Vol. 18, No. 4, 1992, pp. 327-347.

[19]Miller, J. A., Mitchell, R. E., Smooke, M. D., and Kee, R. J., "Toward a comprehensive chemical kinetic mechanism for the oxidation of Acetylene: Comparison model predictions with results from flame and shock tube experiments," *Proceedings of the Nineteenth Symposium (International) on Combustion*, Combustion Institute, Pittsburgh, PA, 1982, pp. 181-196.

Table 1. Simple hydrogen-oxygen mechanism. The species are H_2, O_2, H, O, OH, and H_2O.

j	Reaction	A_j $(cm^3/mol/s/K^{\beta_j})$	β_j	E_j (cal/mol)
1	$H + O_2 \longrightarrow O + OH$	9.76×10^3	0.0	14842.5
2	$O + OH \longrightarrow O_2 + H$	3.26×10^{11}	0.375	−2208.4
3	$O + H_2 \longrightarrow OH + H$	5.08×10^4	2.67	6289.3
4	$OH + H \longrightarrow H_2 + O$	2.28×10^4	2.67	4420.6
5	$H + H_2O \longrightarrow OH + H_2$	9.39×10^8	1.52	18367.5
6	$H_2 + OH \longrightarrow H_2O + H$	2.14×10^8	1.52	3447.5
7	$O + H_2 \longrightarrow OH + OH$	4.50×10^4	2.70	14542.7
8	$OH + OH \longrightarrow O + H_2O$	4.33×10^3	2.70	−2484.3

Table 2. Hydrogen-air detailed kinetics mechanism. The species are $H_2, O_2, H, O, OH, HO_2, H_2O_2, H_2O$, and N_2.

j	Reaction	A_j $\left((mol/cm^3)^{1-\sum_{i=1}^{N}\nu'_{ij}}/s/K^{\beta_j}\right)$	β_j	E_j (cal/mol)
1	$H_2 + O_2 \rightleftharpoons OH + OH$	1.70×10^{13}	0.000	47780
2	$OH + H_2 \rightleftharpoons H_2O + H$	1.17×10^9	1.300	3626
3	$H + O_2 \rightleftharpoons OH + O$	5.13×10^{16}	−0.816	16507
4	$O + H_2 \rightleftharpoons OH + H$	1.80×10^{10}	1.000	8826
5	$H + O_2 + M \rightleftharpoons HO_2 + M$	2.10×10^{18}	−1.000	0
6	$H + O_2 + O_2 \rightleftharpoons HO_2 + O_2$	6.70×10^{19}	−1.420	0
7	$H + O_2 + N_2 \rightleftharpoons HO_2 + N_2$	6.70×10^{19}	−1.420	0
8	$OH + HO_2 \rightleftharpoons H_2O + O_2$	5.00×10^{13}	0.000	1000
9	$H + HO_2 \rightleftharpoons OH + OH$	2.50×10^{14}	0.000	1900
10	$O + HO_2 \rightleftharpoons O_2 + OH$	4.80×10^{13}	0.000	1000
11	$OH + OH \rightleftharpoons O + H_2O$	6.00×10^8	1.300	0
12	$H_2 + M \rightleftharpoons H + H + M$	2.23×10^{12}	0.500	92600
13	$O_2 + M \rightleftharpoons O + O + M$	1.85×10^{11}	0.500	95560
14	$H + OH + M \rightleftharpoons H_2O + M$	7.50×10^{23}	−2.600	0
15	$H + HO_2 \rightleftharpoons H_2 + O_2$	2.50×10^{13}	0.000	700
16	$HO_2 + HO_2 \rightleftharpoons H_2O_2 + O_2$	2.00×10^{12}	0.000	0
17	$H_2O_2 + M \rightleftharpoons OH + OH + M$	1.30×10^{17}	0.000	45500
18	$H_2O_2 + H \rightleftharpoons HO_2 + H_2$	1.60×10^{12}	0.000	3800
19	$H_2O_2 + OH \rightleftharpoons H_2O + HO_2$	1.00×10^{13}	0.000	1800

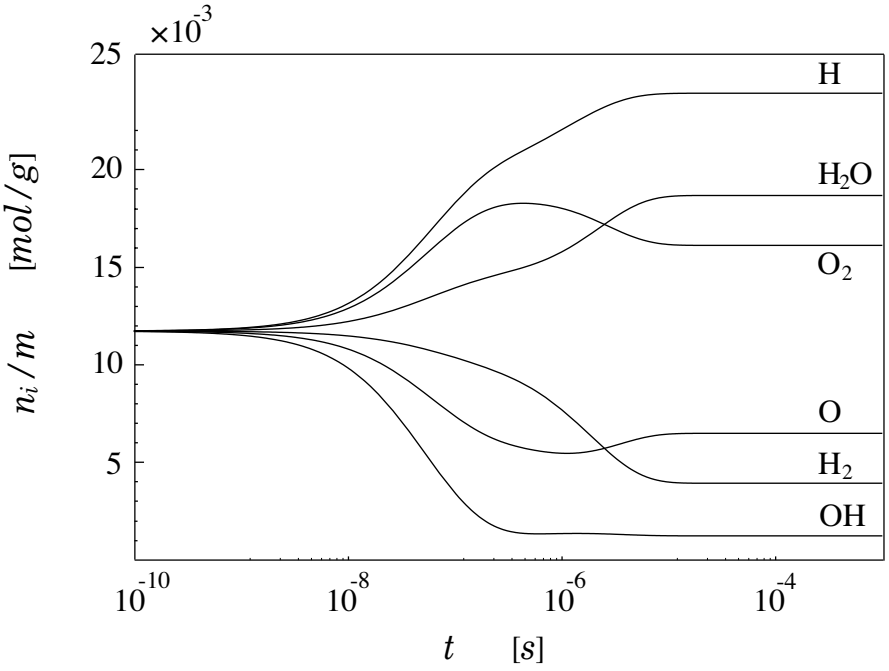

Figure 1. The species time evolution for the simple hydrogen-oxygen mechanism.

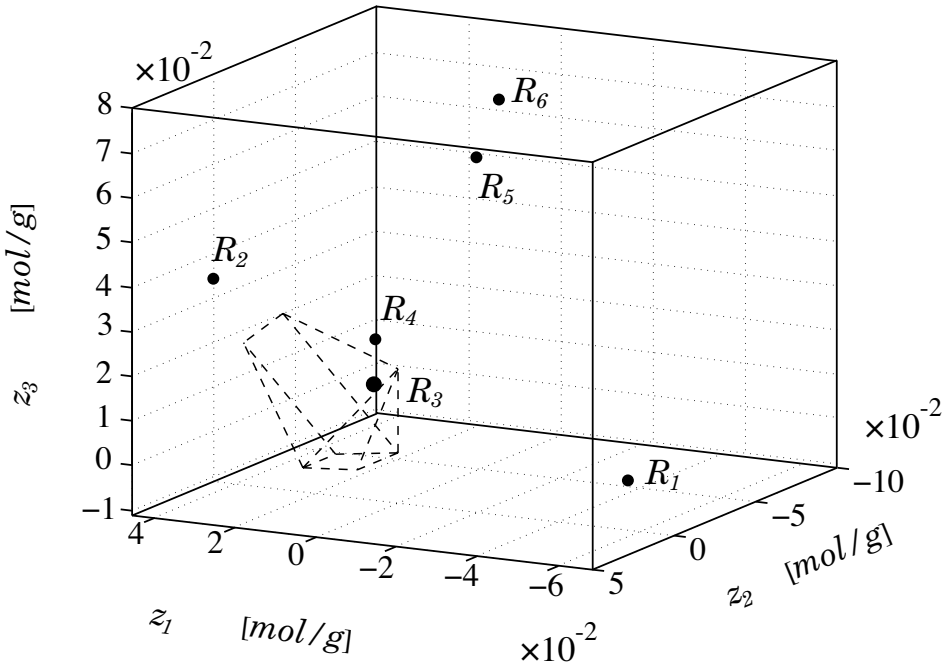

Figure 2. Part of the finite composition space for the simple hydrogen-oxygen mechanism. The critical point R_3 represents the physical equilibrium state for this system, the other critical points are finite but non-physical, and the dashed polygon represents the boundaries of the physically accessible domain of the system.

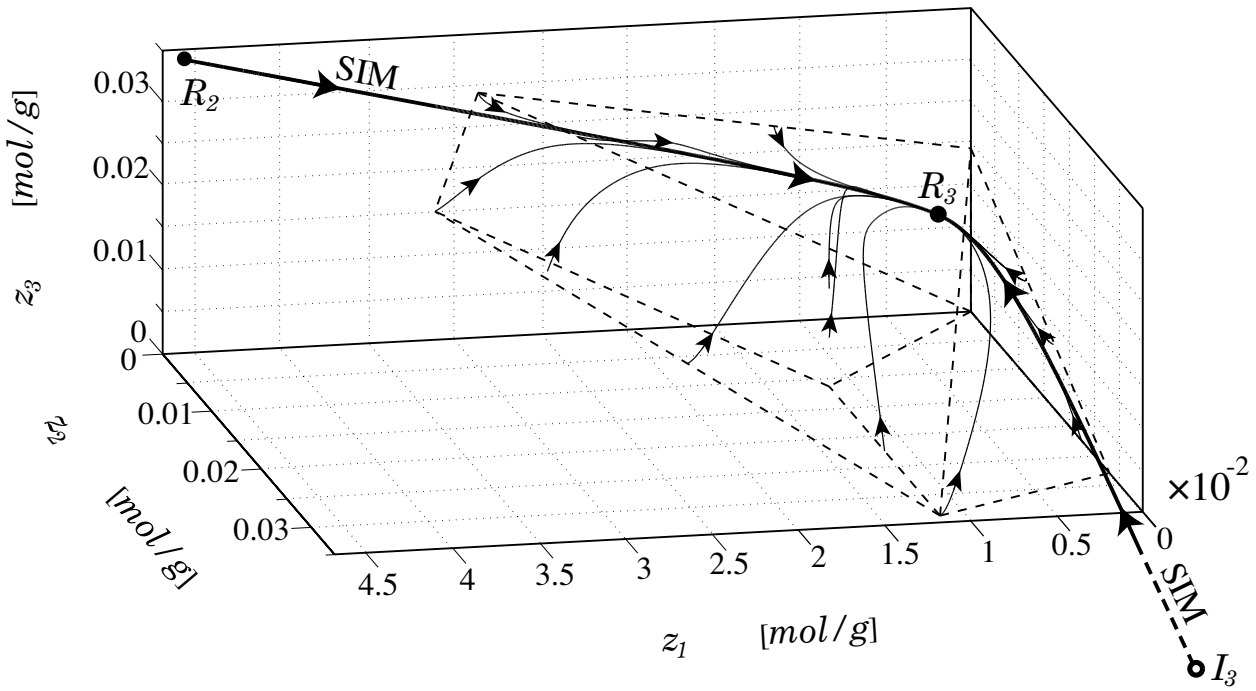

Figure 3. The slow invariant manifold for the simple hydrogen-oxygen mechanism is represented by the thick line. The solid circles represent finite critical points, the open circle represents the infinite equilibrium, and the thin lines are selected trajectories.

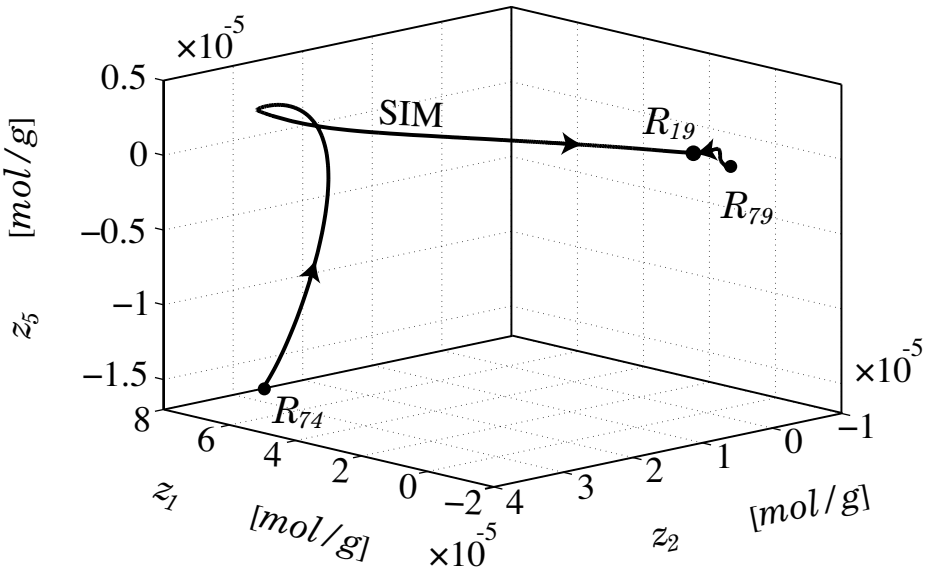

Figure 4. The one-dimensional slow invariant manifold for the detailed hydrogen-air reactive system.